Journal of Photochemistry and Photobiology A: Chemistry 227 (2012) 18–24

Contents lists available at SciVerse ScienceDirect

Journal of Photochemistry and Photobiology A: Chemistry

journal homepage: www.elsevier.com/locate/jphotochem

Photochemistry synthesis. Part 2: Enantiomerically pure polyhydroxy-1,1,3-triarylpropan-2-ols☆

Anke Wilhelm-Mouton[a], Susan L. Bonnet[a], Yuanqing Ding[b], Xing-Cong Li[c], Daneel Ferreira[c,d], Jan H. van der Westhuizen[a,*]

[a] Department of Chemistry, University of the Free State, Nelson Mandela Avenue, Bloemfontein 9301, South Africa
[b] National Center for Natural Products Research, The University of Mississippi, MS 38677, USA
[c] Research Institute of Pharmaceutical Sciences, The University of Mississippi, MS 38677, USA
[d] Department of Pharmacognosy, The University of Mississippi, MS 38677, USA

ARTICLE INFO

Article history:
Received 20 July 2011
Received in revised form 20 October 2011
Accepted 22 October 2011
Available online 29 October 2011

Keywords:
Photochemistry
Flavan-3-ol
Polyhydroxy-1,1,3-triarylpropan-2-ols
Electronic circular dichroism

ABSTRACT

A new method to open the heterocyclic ring of flavan-3-ols *via* photolytic cleavage of the ether bond, with stereoselective trapping of the intermediates with phloroglucinol to obtain phloroglucinol grafted derivatives of flavan-3-ols, was developed. Photolysis of catechin and epicatechin, respectively, in the presence of phloroglucinol yielded the enantiomeric (1S,2S)- and (1R,2R)-1,3-di(2,4,6-trihydroxyphenyl)-1-(3,4-dihydroxyphenyl)propan-2-ols, respectively. The absolute configuration at C-1 and C-2 was determined by electronic circular dichroism (experimental and calculated) and these results confirmed that the trapping mechanism is controlled by the C-3 configuration of the flavan-3-ol.

1. Introduction

Flavan-3-ols and their oligomers are ubiquitous in higher plants [1,2] and are commercially important constituents of red wine [3], leather [4], adhesives [5–7] and black tea [2]. Due to their antioxidant properties, free phenolic flavan-3-ols exhibit protection from diseases attributed to oxidative stress such as cancers [8,9], cardiovascular [10] and neurogenerative diseases [11]. Other biological effects include antitumor activity [12], improved blood flow [13], the inhibition of cholesterol absorption [14] and protection from damage by ultraviolet B radiation [15].

Much of the chemistry and photochemistry of catechin **1a** are explained by the formation of reactive B-ring quinone methide intermediates, e.g. **2a**, or A-ring *o*- or *p*-quinone methide intermediates, e.g. **3** and **4**, respectively [Scheme 1] [16].

Van der Westhuizen and coworkers [17] investigated the photochemistry and electronic circular dichroism (ECD) of enantiomerically pure free phenolic 4-arylflavan-3-ols. Sensitized photolysis (0.05 M benzophenone) of the 4α-phloroglucinol-fisetinidol **5** in methanol gave the first access to the 4β-resorcinol-*ent*-epicatechin **7** and trace amounts of the 4β-phloroglucinol-fisetinidol **9** [Scheme 2].

The formation of compound **7** requires cleavage of the C-2 ether bond to form the B-ring quinone methide **6** followed by stereoselective intramolecular recyclization *via* the stronger nucleophylic hydroxy group of the phloroglucinol D-ring. Inversion of configuration at C-4 from 4α to 4β is due to rotation about the C-2-C-3 bond in **6** (interconversion of the A and D-rings). Inversion of configuration at C-2 from 2*R* to 2*S* is attributed to the C-3 absolute configuration of **5** (C-2 of **6**) that requires *anti*-recyclization of **6**.

Intramolecular recyclization is slow enough to permit bond rotation to yield the observed isomerization at C-2, but too fast to allow intermolecular trapping of intermediate **6** by methanol or 2-propanol. The formation of **9** requires the formation of the A-ring quinone methide **8**. An ionic or radical mechanism could not be ruled out for the formation of **7** but could not explain the formation of **9**. This reaction represented the first and hitherto only synthetic access to the thermodynamically less stable 2,3-*cis*-3,4-*cis*-4-arylflavan-3-ols.

Forest and coworkers [15] investigated the photochemistry of catechin **1a** and epicatechin **10** in water to understand the photochemistry of humic substances in aquatic systems. They observed ultraviolet light induced epimerization of epicatechin **10** and *ent*-catechin **11** in a 1:1 mixture of water and acetonitrile [Scheme 3] to a photostationary ratio of 1:19. This ratio correlates with the fact that 2,3-*trans*-flavan-3-ols are thermodynamically more stable

☆ Part 1 is: Z. Han, S.L. Bonnet, J.H. Van der Westhuizen, Tetrahedron 64 (2008) 2619–2625.

* Corresponding author. Tel.: +27 51 401 2782; fax: +27 51 444 6384.
E-mail address: vdwestjh@ufs.ac.za (J.H. van der Westhuizen).

1010-6030/$ – see front matter © 2011 Elsevier B.V. All rights reserved.
doi:10.1016/j.jphotochem.2011.10.019

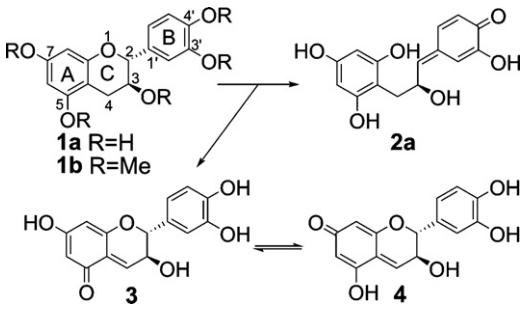

Scheme 1. Formation of *o*- and *p*-quinone methides.

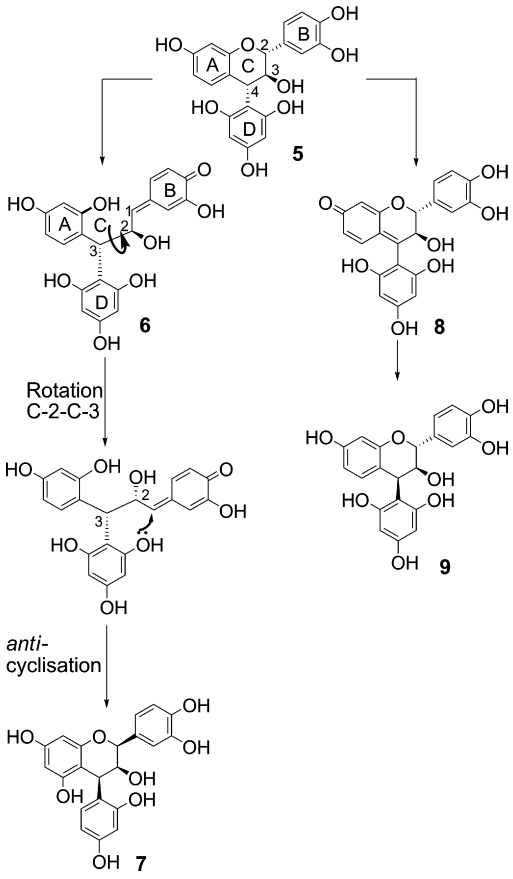

Scheme 2. Photolysis of 4α-phloroglucinol-fisetinidol.

than the 2,3-*cis* diastereomers. Since the absorption coefficients of **10** and **11** are identical, the correlation suggests that photoisomerisation of **10** and **11** takes place *via* the same quinone methide, zwitterionic or biradical intermediate. The sunscreen properties of catechin and epicatechin were attributed to this epimerization.

Mayer and coworkers [18] reported acid-catalyzed [HCl (*aq*)] fission of the heterocyclic ring of catechin **1a** with simultaneous grafting of a nucleophilic phenolic species such as phloroglucinol **12a** followed by dehydration to yield a 2-benzyl-

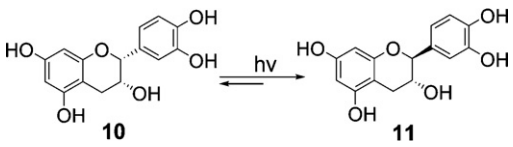

Scheme 3. Photochemical isomerization of epicatechin **10** and *ent*-catechin **11**.

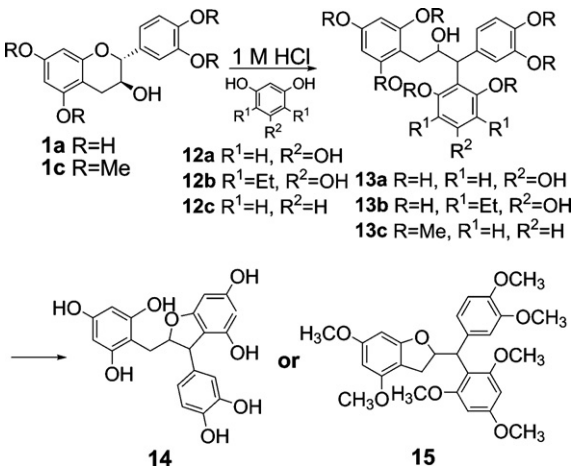

Scheme 4. Acid catalyzed condensation of catechin **1a** with phloroglucinol **12a** and resorcinol **12c**, respectively.

3-phenyl-2,3-dihydrobenzofuran **14** [Scheme 4]. The postulated 1,1,3-triphenylpropanol intermediate **13a** was proven during acid catalyzed condensation of catechin **1a** and diethylphloroglucinol **12b** to yield **13b**. The stereochemistry of the product was not determined.

Weinges and coworkers [19] investigated the acid-catalyzed condensation of tetra-*O*-methylcatechin **1c** and resorcinol **12c** (dioxane/HCl(c); 2:3, v/v). The reaction yielded the 1,1,3-triphenylpropanol **13c** and a 2-diphenylmethyl-2,3-dihydrobenzofuran **15** after methylation [Scheme 4].

Laks et al. [20] found that when catechin **1a** was dissolved in an alkaline solution under mild conditions (ambient temperature, pH 12) in the presence of phloroglucinol **12a**, a mixture of catechinic acid **16** and the phloroglucinol adduct **13a** was formed [Scheme 5]. Catechinic acid **16** is formed *via* nucleophilic attack of the phloroglucinol A-ring on the B-ring quinone methide *via* C-8.

Mitsunaga and co-workers [21–23] reported a BF_3-catalyzed condensation between phenol **17** and catechin **1a** that yielded an acyclic phenolated product **18** and the corresponding dehydration product **19** [Scheme 6].

Herein, we report the photolytic cleavage of the pyran heterocycle of catechin **1a** and epicatechin **10**, and the stereoselective trapping of the intermediates with phloroglucinol **12a** to obtain synthetic access to enantiopure polyhydroxy-1,1,3-triarylpropan-2-ols. We determined the absolute configuration of the 1,1,3-triarylpropan-2-ols *via* the comparison of calculated and experimental ECD spectra.

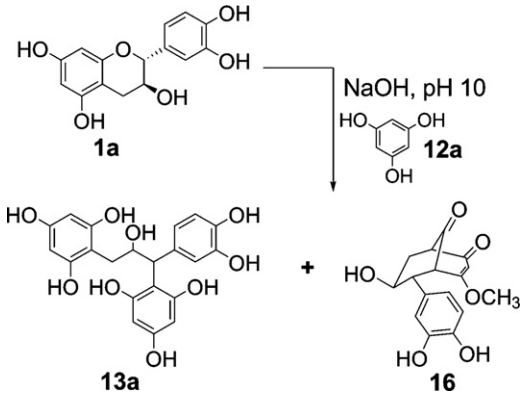

Scheme 5. Base-catalyzed condensation of catechin **1a** with phloroglucinol **12a**.

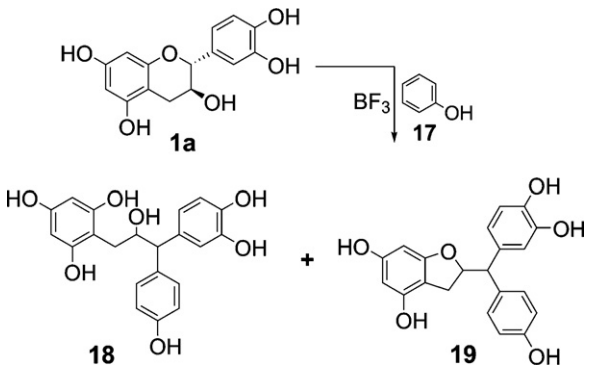

Scheme 6. BF_3 catalyzed condensation between phenol **17** and catechin **1a**.

2. Experimental

2.1. Analytical

All NMR experiments were recorded on a Bruker 600 MHz spectrometer. ECD spectra were recorded on a Jasco J-710 spectropolarimeter in spectrophotometric grade methanol (~1 mg/10 mL MeOH). Mass spectra were recorded on a Waters Quattro Ultima triple quadrupole mass spectrometer, operated in the positive mode. Solid state FR-IR spectra were recorded as KBr pellets on a Bruker Tensor 27 spectrometer in the range of 3000–600 cm^{-1}. All photochemical reactions were carried out inside a RAYON photochemical reactor manufactured by Southern N.E. Ultraviolet Co., Middletown, CT, USA, equipped with Rayonet Photochemical Reactor lamps Cat. No. RPR-250, 300, and 350 nm, respectively.

2.2. Synthesis

2.2.1. Photolysis of catechin

(1S,2S)-1,3-Di(2,4,6-trihydroxyphenyl)-1-(3,4-dihydroxyphenyl)propan-2-ol ***20a****, 2-[(2S,3R)-3-(3,4-dihydroxyphenyl)-2-hydroxy-3-methoxypropyl]benzene-1,3,5-triol* ***21a,*** *and 2-[(2S,3S)-3-(3,4-dihydroxyphenyl)-2-hydroxy-3-methoxypropyl]benzene-1,3,5-triol* ***21c.***

Catechin **1a** (450 mg, 1.55 mmol) and phloroglucinol **12a** (600 mg, 4.74 mmol) were irradiated in MeOH (40 mL) at 250 nm for 20 h. The solvent was evaporated *in vacuo* to give the crude product, which was purified by column chromatography (Sephadex LH-20, EtOH as eluant) to give **20a** (95 mg, 15%) as an amorphous solid, a mixture of **21a** and **21c** (75 mg, 15% combined yield), and unreacted catechin **1a** (155 mg, 34%).

20a: δ_H (600 MHz, DMSO, Me_4Si, 120 °C) 8.93 (1H, s, 1× OH), 8.87 (1H, s, 1× OH), 8.80 (2H, s, 2× OH), 8.74 (1H, s, 1× OH), 8.47 (1H, s, 1× OH), 8.38 (1H, s, 1× OH), 6.61 (1H, d, J = 2.0 Hz, H-2‴), 6.53 (1H, d, J = 8.3 Hz, H-5‴), 6.50 (1H, dd, J = 2.0, 8.3 Hz, H-6‴), 5.85 (2H, s, H-3′, H-5′), 5.84 (2H, s, H-3″, H-5″), 4.58 (1H, d, J = 4.3 Hz, H-1), 4.54 (1H, m, H-2), 2.70 (1H, dd, J = 2.5 Hz, 14.3 Hz, H-3α), 2.43 (1H, dd, J = 9.6 Hz, 14.3 Hz, H-3β); δ_C (100.6 MHz, Act-D_6) 157.5, 157.2, 157.0, 156.9 (6× C-OH), 144.4, 142.9 (2× C-OH), 134.3 (C-1‴), 119.5 (C-2‴), 115.6 (C-5‴), 114.6 (C-6‴), 105.7 (C-1″), 104.8 (C-1′), 95.2 (C-3′/5′ and C-3″/5″), 76.6 (C-2), 45.4 (C-1), 29.3 (C-3); m/z (ESI) 417 (30, MH^+), 257 (25), 159 (100), 141 (50), 109 (37); HR-MS: $[M+H]^+$, found m/z 417.1189. $C_{21}H_{20}O_9$ requires m/z 417.1185; IR (KBr): υ max = 3419, 1614, 1151, 1023, 989 cm^{-1}; ECD: $[\theta]_{286.6}$ 8.3×10^2, $[\theta]_{262.6}$ 6.3×10^2, $[\theta]_{248.0}$ 3.0×10^2, $[\theta]_{239.0}$ -2.2×10^2, $[\theta]_{220.4}$ 3.9×10^3, $[\theta]_{207.8}$ -3.4×10^2, $[\theta]_{201.6}$ 3.3×10^2, $[\theta]_{190.4}$ 1.7×10^2.

Acetylation of **20a** yielded *(1S,2S)-1,3-di(2,4,6-triacetoxyphenyl)-1-(3,4-diacetoxyphenyl)propan-2-ol* ***20b***.

20b: δ_H (600 MHz, $CDCl_3$, Me_4Si) 7.19 (1H, d, J = 2.0 Hz, H-2‴), 7.17 (1H, dd, J = 2.0, 8.5 Hz, H-6‴), 7.10 (1H, d, J = 8.5 Hz, H-5‴), 6.85 (2H, s, H-3″, H-5″), 6.82 (2H, broad s, H-3′, H-5′), 5.84 (1H, m, H-2), 4.75 (1H, d, J = 9.0 Hz, H-1), 3.19 (1H, dd, J = 5.7, 14.4 Hz, H-3α), 3.00 (1H, dd, J = 4.6, 14.4 Hz, H-3β), 2.27 (3H, s, 1× OAc), 2.26 (3H, s, 1× OAc), 2.25 (3H, s, 1× OAc), 2.23 (3H, s, 1× OAc), 2.04 (6H, broad s, 2× OAc), 2.00 (6H, s, 2× OAc), 1.72 (3H, s, 1× OAc); δ_C (150 MHz, $CDCl_3$, Me_4Si) 170.6–168.0 (9× O-**C**OCH_3), 150.5 (C-3″/C-5″), 149.6 (C-3′/C-5′), 149.3 (C-3‴), 149.2 (C-4′), 142.0 (C-4″), 140.6 (C-4‴), 138.2 (C-1′), 126.2 (C-2‴), 123.5 (C-5‴), 123.0 (C-1″), 122.8 (C-6‴), 118.8 (C-1‴), 114.3 (C-2′/C-6′), 113.7 (C-2″/C-6″), 71.2 (C-2), 42.1 (C-3α/β), 26.1 (C-1), 21.1–20.3 (9× O-CO**C**H_3).; HR-MS: $[M+H]^+$, found m/z 795.2139. $C_{39}H_{38}O_{18}$ requires m/z 795.2135.; IR (KBr): υ max = 1774, 1371, 1193, 1025 cm^{-1}; ECD: $[\theta]_{278.4}$ 2.4×10^3, $[\theta]_{260.0}$ 1.6×10^3, $[\theta]_{230.0}$ 4×10^3, $[\theta]_{209.2}$ 8.7×10^3, $[\theta]_{193.0}$ -9.4×10^1, $[\theta]_{187.0}$ 1.5×10^3.

2-[(2S,3R)-2-Acetoxy-3-(3,4-diacetoxyphenyl)-3-methoxypropyl] benzene-1,3,5-triyl triacetate ***21b****, and 2-[(2S,3S)-2-acetoxy-3-(3,4-diacetoxyphenyl)-3-methoxypropyl]benzene-1,3,5-triyl triacetate* ***21d****.*

Acetylation of the reaction mixture yielded **21b** and **21d** as a mixture which could not be separated. However, since there is almost no overlap of resonances in the ^1H and ^{13}C NMR spectra, respectively, both acetate diastereoisomers could be fully characterized with NMR.

21b (in mixture): δ_H (600 MHz, $CDCl_3$, Me_4Si) 7.10 (1H, d, J = 8.2 Hz, H-5′), 7.06 (1H, d, J = 2.0 Hz, H-2′), 7.03 (1H, dd, J = 2.0, 8.2 Hz, H-6′), 6.87 (2H, s, H-3″/H-5″), 5.06 (1H, m, H-2), 4.12 (1H, d, J = 3.7 Hz, H-3), 3.23 (3H, s, 1× OMe), 2.85 (1H, dd, J = 6.7, 13.8 Hz, H-1α), 2.61 (1H, dd, J = 8.2, 13.8 Hz, H-1β), 2.20 (3H, s, 1× OAc), 2.21 (3H, s, 1× OAc), 2.19 (6H, s, 2× OAc), 2.18 (3H, s, 1× OAc), 1.85 (3H, s, 1× OAc); δ_C (100.6 MHz, $CDCl_3$) 170.2–167.9 (6× O-**C**OCH_3), 150.2–141.7 (C-2″/C-6″, C-4″, C-3′, C-4′), 136.5 (C-1″), 125.3–122.5 (C-2′, C-5′, C-6′), 199.7 (C-1′), 113.9 (C-3″/C-5″), 81.1 (C-3), 74.1 (C-2), 57.6 (O**C**H_3), 24.7 (C-1), 21.2–20.5 (6× O-CO**C**H_3).

21d (in mixture): δ_H (600 MHz, $CDCl_3$, Me_4Si) 7.21 (1H, dd, J = 2.0, 8.3 Hz, H-6′), 7.15 (1H, d, J = 2.0 Hz, H-2′), 7.13 (1H, d, J = 8.3 Hz, H-5′), 6.75 (2H, s, H-3″/H-5″), 5.00 (1H, m, H-2), 4.33 (1H, d, J = 3.5, H-3), 3.28 (3H, s, 1× OMe), 3.00 (1H, dd, J = 10.9, 14.3 Hz, H-1α), 2.53 (1H, dd, J = 2.90, 14.3 Hz, H-1β), 2.16 (3H, s, 1× OAc), 2.15 (3H, s, 1× OAc), 2.07 (3H, s, 1× OAc), 2.05 (6H, s, 2× OAc), 2.03 (3H, s, 1× OAc); δ_C (100.6 MHz, $CDCl_3$) 170.2–167.9 (6× O-**C**OCH_3), 150.2–141.7 (C-2″/C-6″, C-4″, C-3′, C-4′), 137.0 (C-1″), 125.0–122.3 (C-2′, C-5′, C-6′), 120.0 (C-1′), 113.6 (C-3″/C-5″), 83.6 (C-3), 76.1 (C-2), 58.0 (O**C**H_3), 22.9 (C-1), 21.2–20.5 (6× O-CO**C**H_3).

2.2.2. Photolysis of epicatechin

(1R,2R)-1,3-Di(2,4,6-trihydroxyphenyl)-1-(3,4-dihydroxyphenyl)propan-2-ol ***22a****.*

Epicatechin **10** (580 mg, 2.0 mmol) and phloroglucinol **12a** (750 mg, 5.95 mmol) were irradiated at 250 nm in MeOH (40 mL) under nitrogen for 20 h. The solvent was evaporated *in vacuo* to give the crude product, which was purified by column chromatography (Sephadex LH-20, ethanol as eluant) to give the *title compound* **22a** (137 mg, 16%) as an amorphous solid, *ent*-catechin (58 mg, 10%) [ECD spectra of acetylated catechin and *ent*-catechin Figs. S2 and S3, respectively], and unreacted epicatechin **10** (181 mg, 31%).

22a: δ_H (600 MHz, DMSO, Me_4Si) identical to **20a**. δ_C (100.6 MHz, $CDCl_3$) identical to **20a**. HR-MS: $[M+H]^+$, found m/z 417.1194. $C_{21}H_{20}O_9$ requires m/z 417.1185. IR (KBr): υ max = 3419, 1614, 1151, 1023, 989 cm^{-1}; ECD: $[\theta]_{293.8}$ 6.8×10^2, $[\theta]_{276.6}$ 8.6×10^2, $[\theta]_{260.0}$ -2.6×10^2, $[\theta]_{238.2}$ 6.9×10^2, $[\theta]_{222.2}$ -3.8×10^3, $[\theta]_{206.8}$ 1.2×10^3, $[\theta]_{199.8}$ -4.1×10^2, $[\theta]_{188.0}$ 5.1×10^2.

Acetylation of ***22a*** *yielded (1R,2R)-1,3-di(2,4,6-triacetoxyphenyl)-1-(3,4-diacetoxyphenyl)propan-2-ol* ***22b****.*

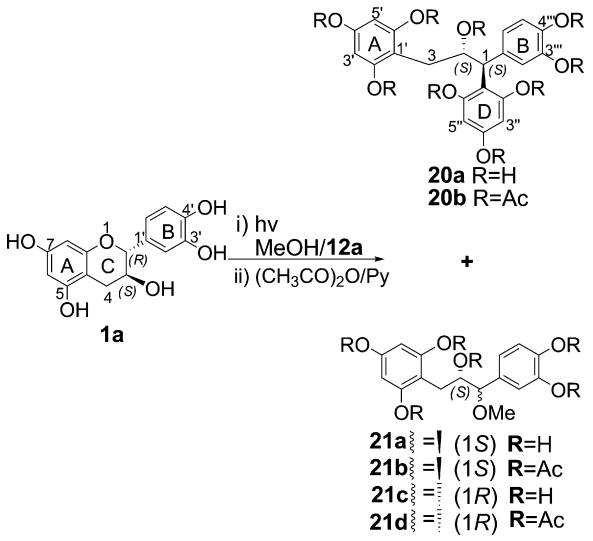

Scheme 7. Photolysis of catechin **1a** and phloroglucinol **12a**.

22b: δ_H (600 MHz, $CDCl_3$, Me_4Si) identical to **20b**. δ_C (150 MHz, $CDCl_3$, Me_4Si) identical to **20b**. HR-MS: $[M+H]^+$, found *m/z* 795.2145. $C_{39}H_{38}O_{18}$ requires *m/z* 795.2135. IR (KBr): υ max identical to **20b**; ECD: $[\theta]_{292.4}$ 2.3×10^3, $[\theta]_{251.4}$ 8.7×10^2, $[\theta]_{230.4}$ -2.7×10^3, $[\theta]_{209.6}$ -9.0×10^3, $[\theta]_{195.8}$ 2.3×10^3, $[\theta]_{185.2}$ 6×10^2.

*2.2.3. Photolysis of 3′,4′,5,7-tetra-O-methylcatechin 2-(2-Hydroxy-2-methylpropyl)-3,5-dimethoxyphenol **25**.*

3′,4′,5,7-Tetra-*O*-methylcatechin **1c** (50 mg, 0.14 mmol) and phloroglucinol **12a** (82 mg; 0.65 mmol) in MeOH/acetone (25 mL) (90/10, v/v) were irradiated at 300 nm for 2.5 h. The solvent was evaporated *in vacuo* to give the crude product, which was purified by silica column chromatography (T/A 7:3) to give the *title compound* **25** (7.0 mg, 14%) as an amorphous solid; R_f (T/A 7:3) 0.60, and 3,4-dimethoxybenzaldehyde **24** (4.0 mg, 8%); R_f (T/A 7:3) 0.46.

25: δ_H (600 MHz, $CDCl_3$, Me_4Si) 8.48 (1H, s, OH-1), 6.18 (1H, d, *J* = 2.4 Hz, H-3), 6.08 (1H, d, *J* = 2.4 Hz, H-5), 3.77 (3H, s, OMe), 3.75 (3H, s, OMe), 2.82 (2H, s, CH2), 1.94 (1H, s, OH-2′), 1.28 (6H, s, 2×-CH3). δ_C (150 MHz, $CDCl_3$, Me_4Si) 159.84 (C-2), 159.29 (C-4), 157.54 (C-6), 106.05 (C-1), 94.56 (C-3), 91.17 (C-5), 75.25 (C-2′), 55.53, 55.25 (2×-O**C**H3), 35.74 (C-1′), 29.26 (C-3′); HR-MS: $[M+H]^+$, found *m/z* 227.1287. $C_{12}H_{18}O_4$ requires *m/z* 227.1283.

3. Results

Photolysis of catechin **1a** in MeOH at 250 nm in the presence of phloroglucinol **12a** resulted in the isolation of the optically active product **20a** (15% yield) with a (1*S*,2*S*) configuration, and unreacted optically active starting material **1a** (34%) [Scheme 7]. Two side products, diastereoisomers **21b** and **21d**, were detected upon acetylation of the reaction mixture, but could not be separated. Since there is no overlap of resonances, the ^{1}H NMR spectrum of the mixture could be interpreted. The ratio of **21b**:**21d** was 4:1 (yields of 12% and 3%, respectively).

Photolysis of epicatechin **10** under the same conditions resulted in the isolation of the optically active products **22a** (15% yield) and *ent*-catechin **11**, in a 2:1 ratio, and unreacted optically active starting material **10** (25%) [Scheme 8].

Photolysis of 3′,4′,5,7-tetra-*O*-methylcatechin **1c** in MeOH and in the presence of 5 eq. of phloroglucinol gave no products. Addition of acetone (10%), a triplet sensitizer, to the reaction mixture leads to the formation of fragmentation products **24** (8%) and **25** (15%) [Scheme 9].

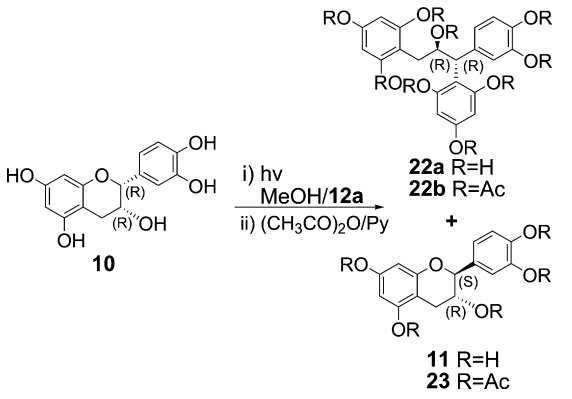

Scheme 8. Photolysis of epicatechin **10** and phloroglucinol **12a**.

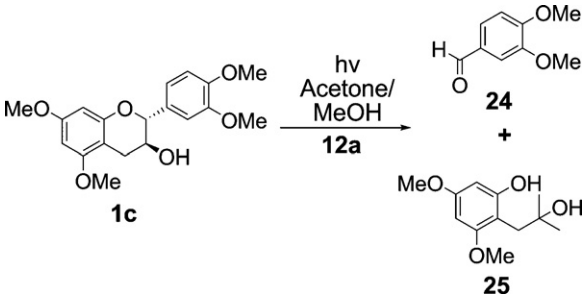

Scheme 9. Photolysis of tetra-*O*-methylcatechin **1c** in MeOH/Acetone.

Photolysis of catechin **1a** and epicatechin **10** in the presence of resorcinol and phenol, respectively, at 250 nm showed no coupling products. Grafting of a phenolic moiety at C-2 of the presumed B-ring quinone-methide intermediate (e.g. **2a)** was only observed in the case of phloroglucinol.

4. Discussion

The respective 1,1,3-triarylpropan-2-ols **20a** and **22a**, obtained from photolysis of catechin **1a** and epicatechin **10** in the presence of phloroglucinol, have identical ^{1}H NMR spectra, but mirror image ECD spectra. The pronounced mirror image Cotton effects observed for **20a** and **22a** in the 215–280 nm region, indicate their enantiomeric relationship [Fig. 1].

The aromatic region of the ^{1}H NMR spectra of the enantiomers **20a** and **22a** show one two-proton singlet at δ 5.84 for the free-rotating phloroglucinol moiety (A-ring), one ABX system corresponding to the B-ring (δ 6.48–6.64), and two broadened singlets at δ 5.82 and 5.90 indicating the two protons of the rotationally restricted [20] D-ring phloroglucinol moiety. At 120 °C the H-3(D)

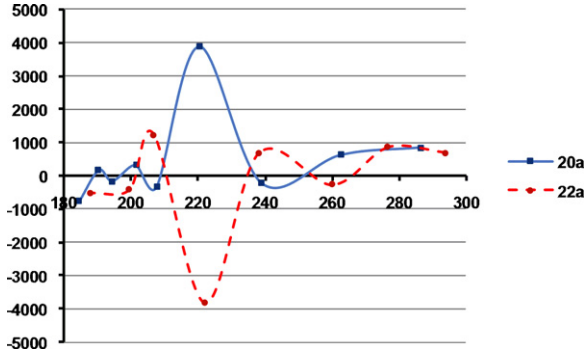

Fig. 1. ECD spectra of **20a** and **22a**.

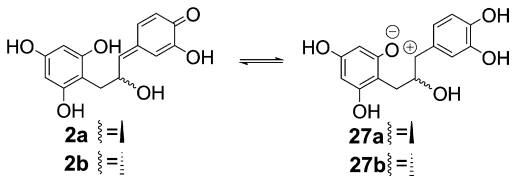

Fig. 2. Quinone methide **2a** and **b** and ionic intermediate **27a** and **b** tautomers.

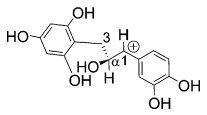

Fig. 3. α-Hydrogen atom occupies the 1,3-allylic-strain position.

and H-5(D) resonances coalesce into a sharp two-proton singlet at δ 5.85. In the aliphatic region H-1 and H-2 overlap at δ 4.46 at room temperature. At 120 °C H-1 appears as a doublet at δ 4.58 (J = 4.3 Hz) and H-2 as a multiplet at δ 4.50–4.46. One of the diastereotopic C-3 protons resonates as a doublet of doublets at δ 2.43 (J = 9.6, 14.3 Hz), while the resonance of the other proton overlaps with the DMSO resonance at δ 5.84.

Acetylation of **20a** and **22a** yielded the enantiomers **20b** and **22b**, respectively. The presence of nine acetoxy resonances in their ^{1}H NMR spectra, confirms the fission of the heterocyclic C-rings and the addition of a phloroglucinol moiety at C-1. The shielded acetoxy resonances (δ 1.72) for **20b** and **22b** correspond to the C-2 acetoxy group. The HMBC spectra show a correlation between H-1 (δ 4.46) and C-1(D) (δ 26.2) indicating that the additional phloroglucinol rings are indeed attached to C-1.

Photolysis of epicatechin **10** also resulted in epimerization at C-2 to additionally yield *ent*-catechin **11**. The ^{1}H NMR spectrum of **11** is identical to that of catechin **1a**, but mirror image ECD spectra shows their enantiomeric relationship [24]. The photolytic epimerization at C-2 of catechin **1a** to the thermodynamically less stable *ent*-epicatechin is not observed upon monitoring the reaction *via* TLC. This correlates with Forest's conclusion that the 2,3-*trans* isomer (e.g. *ent*-catechin) is thermodynamically more stable than the 2,3-*cis* isomer, epicatechin [15].

The OMe-substituted diastereoisomers **21b** and **21d** appeared as a single band upon preparative TLC. Efforts to further purify the mixture failed. The high-resolution ^{1}H NMR resonances of the mixture do not overlap and occur in a consistent 4:1 ratio permitting the assignment of all the protons of **21b** and **21d**, respectively, in the mixture. The characteristic ABX system of the B-ring is observed in the δ 7.30–7.00 region. Two one-proton doublet of doublets resonate at δ 2.85 and 2.61 for the major product (**21b**), and at δ 3.00 and 2.53 for its isomer (**21d**), and are assigned to the two diastereotopic C-3 methylene protons. The C-1 methoxy group that resonates at δ 3.23 and 3.28, respectively, proves the acyclic nature of the product. The free phenolic OMe-substituted acetate precursors **21a** and **21c** were not isolated.

Identification of the methanol-trapped products (**21a** and **21c**) and not the hydroxymethyl-substituted product **26** that would be expected from a radical mechanism [25], indicates a *p*-hydroxy stabilized benzylic cation **27a** or *p*-quinone methide **2a** intermediate mechanism.

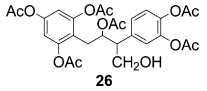

26

We could not distinguish unequivocally between the two putative intermediates **2a** and **27a** [Fig. 2].

Since both are planar C-1 sp^2 hybridized tautomers, we do not expect much difference in thermodynamic stability and stereoselectivity. The pK_a values of phenols in the excited state are lower (more acidic) than in the ground state [26], indicating improved stabilization of an ionic photolytic intermediate in the excited state compared to the ground state. The absence of coupling products in the photolysis of tetra-*O*-methylcatechin **1c**, indicates that a free C-4′ OH is essential to stabilize the intermediate benzylic carbocation or quinone methide [16,27]. Since singlet excited $\pi \rightarrow \pi^*$-states are associated with ionic reaction products and $\pi \rightarrow \pi^*$-triplet states with radical reaction products [28], we postulate a singlet mechanism. This is supported by the observation that efforts to sensitize the reaction with acetophenone or acetone to improve yields failed and that the use of 5 equivalents of phloroglucinol, a known singlet inhibitor, leads to lower yields.

The absolute configuration at C-1 of the phloroglucinol adduct **20a** depends on the face of attack of the nucleophile **12a** at the planar C-1 centre of **2a**/**27a**. Attack at the *Si*-face of **2a**/**27a** will give rise to 1*R* absolute configuration, while *Re*-face attack will yield the 1*S* diastereomer. Bach and coworkers [29] postulated that α-chiral secondary and tertiary benzylic carbocations will display a preferred conformation in which the α-hydrogen atom occupies the 1,3-allylic strain position. The diastereotopic faces of the carbocations are differentiated by the functional groups at the α-carbon. In the case of intermediate **2a**/**27a**, this would imply that the bulkier benzyl group at C-2 and not the less bulky hydroxy group direct attack to the *Si*-face leading to the 1*R*,2*S* diastereomer [Fig. 3].

The C-2 absolute configuration in compound **20a** was established by theoretical calculation of its electronic circular dichroism (ECD) spectrum. A systematic conformational search was carried out with an arbitrarily chosen 1*S*,2*S* absolute configuration *via* Monte Carlo random search in the SYBYL 8.1 program using an MMFF94 molecular mechanics force-field calculation. An energy cutoff of 10 kcal/mol was used to generate a wide window of conformers in the Boltzmann population, affording 77 conformers. The first 20 conformers within an energy cut-off of 4 kcal/mol were geometrically optimized using density functional theory (DFT) at the B3LYP/6-31G** level (gas phase) and 19 conformers were relocated. Six predominant conformers, **20c, 20d**, **20e**, **20f**, **20g**, and **20h** were conformationally analyzed with a Boltzmann distribution of 57.7, 6.6, 8.4, 4.2, 8.0, and 8.7% by relative energy at the B3LYP/6-311++G**//B3LYP/6-31G** level [Fig. 4, Table S1].

Their key dihedral reference angles are shown in Table S3. Time dependent density functional theory (TDDFT) calculations [30–36] of the six conformers were performed at the B3LYP/6-311++G**//B3LYP/6-31G** level (gas phase). The overall pattern of the calculated ECD spectrum is consistent with the experimental one, although a blue shift [35] of approximately 15 nm is observed for the three Cotton effects (207, 223, and 236 nm compared to 221, 239, and 250–262 nm) [Fig. 5], confirming the absolute configuration as 1*S*,2*S*.

This indicates that the nucleophilic attack at C-1 of **2a**/**27a** takes place from the *Re*-face (*anti* to the C-2 hydroxy group). The C-2 hydroxy group and not the bulkier benzyl group directs nucleophilic attack from the *anti*-position.

It appears from the optimized geometry of **20a**, determined to be **20c** [Fig. 4], that the high-amplitude Cotton effect at 221 nm in the experimental ECD spectrum derives from the chiral perturbation of the closely positioned phloroglucinol and catechol chromophores at C-1. The spatial orientation of the two chromophores in **20c** is coincidently similar to that of the 4-aryl moiety relative to the A/C-ring plane of 4β-arylflavan-3-ols (e.g. **9**), which exhibit diagnostic positive Cotton effects at 220–240 nm [36]. Thus, the C-1 absolute configuration in **20a** was confirmed as 1*S*.

Such exclusive formation of the 1*S* diastereoisomer indicates that the directory effect is indeed exerted by the C-2 hydroxy group and not by the C-2 benzyl group.

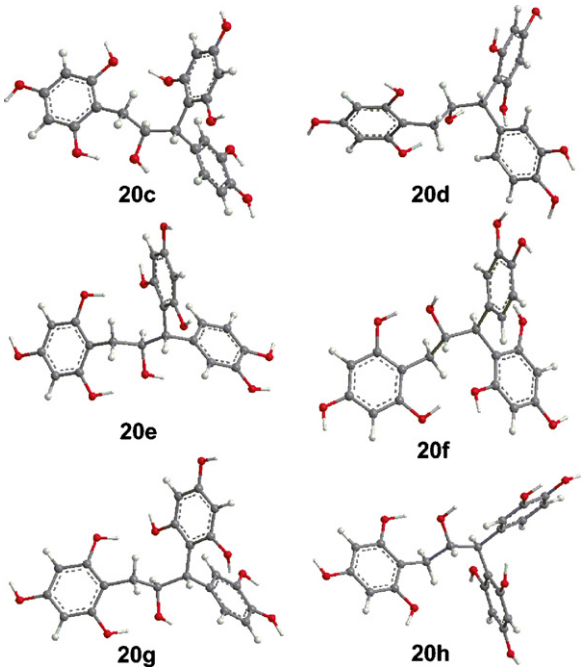

Fig. 4. Optimized geometry of **20a**.

A feasible mechanism for the formation of the 1,1,3-triarylpropan-2-ol **20a** is summarized in Scheme 10. The same mechanism accounts for the formation of the epicatechin derived adduct **22a**.

Thus, heterolytic cleavage of the etherocyclic bond in the singlet excited state **28** leads to formation of the quinone methide **2a**/benzylic carbocation **27a** pair. Stereoselective trapping of these reactive intermediates with phloroglucinol from the face *anti* to the 2-hydroxy group *via* either the quinone methide **2a** or the benzylic carbocation-derived oxirane **29** yields the enantiopure 1,1,3-triarylpropan-2-ol **20a**.

The formation of *ent*-catechin **11** in the photolysis of epicatechin (epimerization at C-2) and the absence of *ent*-epicatechin in the photolysis of catechin (no epimerization at C-2) indicates that recyclization of ring fission intermediates is only feasible from the face *anti* to the 2-hydroxy group. This is in agreement with our conclusion regarding the stereoselectivity of nucleophilic attack by phloroglucinol on **2a** or **27a**.

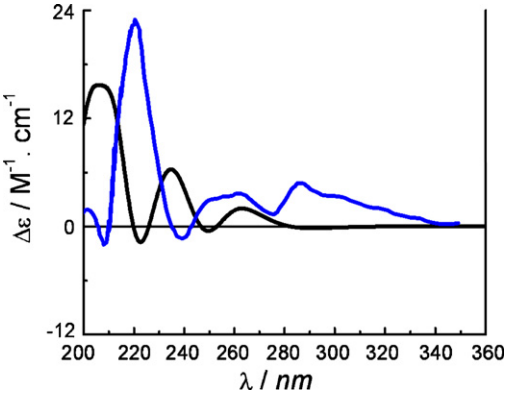

Fig. 5. Calculated ECD spectrum of compound **20a** (black line) at the B3LYP/6-311++G**//B3LYP/6-31G**level (gas phase) and its experimental ECD spectrum (blue line) in MeOH. (For interpretation of the references to color in this figure legend, the reader is referred to the web version of the article.)

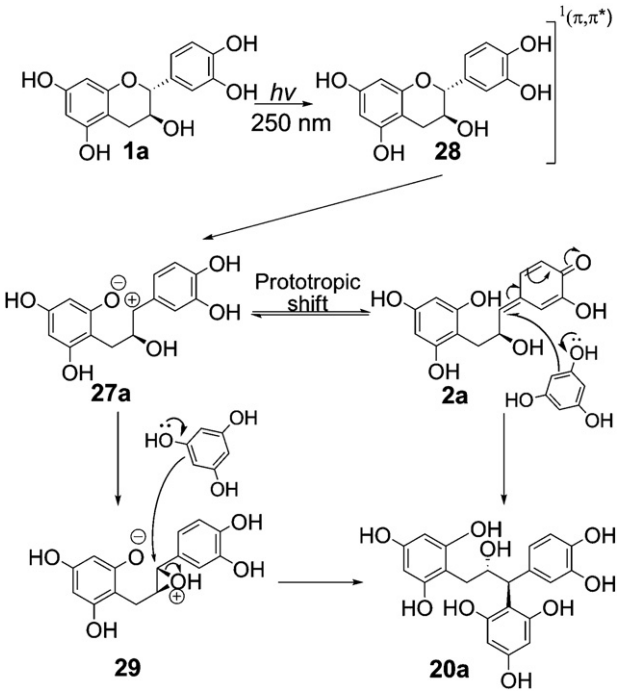

Scheme 10. Proposed mechanism for the formation of the 1,1,3-triarylpropan-2-ol **20a**.

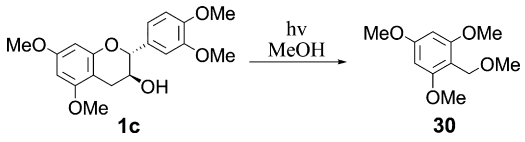

Scheme 11. Photolysis of tetra-*O*-methylcatechin **1c** in pure MeOH.

The formation of both diastereoisomers of the minor MeOH-trapped products **21a** and **21c**, may be attributed to the decreased bulk of MeOH in comparison to that of phloroglucinol. The major isomer **21a** is presumably formed from attack at the *Re*-face of intermediate **2a**/**27a**, while the less favoured *Si*-face-attack afforded **21c**.

Thus, the stereoselectivity of these photolytic reactions may be attributed to the C-2 hydroxy group of the intermediate **2a**/**27a** (for catechin **1a**) or **2b**/**27b** (for epicatechin **10**), respectively, that allows the bulky phloroglucinol group to exclusively attack the quinone methide *anti* to the C-2 hydroxy group for the catechin and epicatechin reaction intermediates **2a**/**27a** and **2b**/**27b**, respectively.

Tetra-*O*-methylcatechin (**1c**) does not undergo photolytic coupling with phloroglucinol under our conditions. This supports the presence of a quinone methide intermediate **2a** in the transformation of **1a** to **20a** (Scheme 10) as **1c** cannot form a B-ring quinone methide. The formation of fragmentation products **24** and **25** in acetone/MeOH expands the work of Fourie and coworkers [27] who observed the formation of **30** when **1c** was irradiated in pure MeOH [Scheme 11]. We assume that the methanol adduct **30** is formed *via* a singlet and thus an ionic mechanism, and the acetone adduct **25** *via* a triplet and radical mechanism.

5. Conclusion

We have developed a novel method to cleave the heterocyclic ring of flavan-3-ols *via* photolytic fission of the ether bond. The intermediates are stereoselectively trapped with phloroglucinol to obtain phloroglucinol-grafted derivatives of flavan-3-ols albeit in moderate yields. It was demonstrated that the trapping mechanism

is controlled by the C-3 configuration of the flavan-3-ol. By judicial choice of starting materials both the (*R*,*R*) and (*S*,*S*) enantiomers of the grafted phloroglucinol products were accessible.

Appendix A. Supplementary data

Supplementary data associated with this article can be found, in the online version, at doi:10.1016/j.jphotochem.2011.10.019.

References

[1] D. Ferreira, D. Slade, J.P.J. Marais, Flavans and proanthocyanidins, in: Ø.M. Anderson, K.R. Markham (Eds.), Flavonoids: Chemistry, Biochemistry and Applications, Taylor & Francis, Boca Raton, 2006, pp. 553–616.
[2] L.J. Porter, J.B. Harborne, The Flavonoids – Advances in Research Since 1986, Chapman & Hall, London, 1994, pp. 23–56.
[3] R. Corder, W. Mullen, N.Q. Khan, S.C. Marx, E.G. Woods, M.J. Carrier, A. Crozier, Oenology: redwine procyanidins and vascular health, Nature 444 (2006) 566.
[4] D.G. Roux, D. Ferreira, J.J. Botha, Structural considerations in predicting the utilization of tannins, J. Agric. Food Chem. 28 (1980) 216–222.
[5] A. Pizzi, Wattle based adhesives for exterior grade particleboard, Forest Prod. J. 28 (1978) 42–47.
[6] M.A.E. Santana, M.G.D. Baumann, A.H. Conner, Resol resins prepared with tannin liquefied in phenol, Holzforschung 49 (1995) 146–152.
[7] N.S. Cetin, N. Ozmen, Use of organosolv lignin in phenol–formaldehyde resins for particleboard production. I. Organosolv lignin modified resins, Int. J. Adhes. Adhes. 22 (2002) 477–480.
[8] J. Jankun, S.H. Selman, R. Swiercz, E. Skrypczak-Jankun, Why drinking green tea could prevent cancer, Nature 387 (1997) 561.
[9] S. Garbisa, S. Biggin, N. Cavallarin, L. Sartor, R. Benelli, A. Albini, Tumor invasion: molecular shears blunted by green tea, Nat. Med. 5 (1999) 1216.
[10] M. De Lorgeril, P. Salen, Wine ethanol, platelets and Mediterranean diet, Lancet 353 (1999) 1067.
[11] M.A Smith, G. Perry, P.L. Richey, L.M. Sayre, V.E. Anderson, M.F. Beal, N. Kowall, Oxidative damage in Alzheimer's, Nature 382 (1996) 120–121.
[12] A.M. Mendoza-Wilson, D. Glossman-Mitnik, Theoretical study of the molecular properties and chemical reactivity of (+)-catechin and (−)-epicatechin related to their antioxidant ability, Mol. Struct.: Theochem. 761 (2006) 97–106.
[13] H. Schroeter, C. Heiss, J. Balzer, P. Kleinbongard, C.L. Keen, K. Hollenberg, H. Sies, C. Kwik-Uribe, H.H. Schmitz, M. Kelm, (−)-Epicatechin mediates beneficial effects of flavanol-rich cocoa on vascular function in humans, Proc. Natl. Acad. Sci. U.S.A. 103 (2006) 1024–1029.
[14] R.E. Kreibich, R.W. Hemingway, Condensed tannin–resorcinol adducts in laminating adhesives, Forest Prod. J. 35 (1985) 23–25.
[15] K. Forest, P. Wan, C.M. Preston, Catechin and hydroxybenzhydrols as models for the environmental photochemistry of tannins and lignins, Photochem. Photobiol. Sci. 3 (2004) 463–472.
[16] P. Wan, D.W. Brousmiche, C.Z. Chen, J. Cole, M. Lukeman, M. Xu, Quinone methide intermediates in organic photochemistry, Pure Appl. Chem. 73 (2001) 529–534.
[17] J.H. Van der Westhuizen, D. Ferreira, D.G.J. Roux, Synthesis of condensed tannins. Part 2. Synthesis of photolytic rearrangement. Stereochemistry, and circular dichroism of the first 2,3-cis-3,4-cis-4-arylflavan-3-ols, J. Chem. Soc. Perkin Trans. I (1981) 1220–1226.
[18] W. Mayer, F. Merger, G. Frank, Uber Kondensationsprodukte der Catechine, VI. Zur Konstitution der Reaktionsprodukte des (+)-Catechins mit Phloroglucin und C-Äthyl-phloroglucin, Liebigs Ann. Chem. 675 (1964) 126–134.
[19] K. Weinges, F. Toribio, Catechin-resorcinol condensation, Liebigs Ann. Chem. 681 (1965) 161–169.
[20] P.E. Laks, R.W. Hemingway, A.H. Conner, Condensed tannins. Base-catalysed reactions of polymeric procyanidins with phloroglucinol: intramolecular rearrangements, J. Chem. Soc. Perkin Trans. I (1987) 1875–1881.
[21] T. Mitsunaga, I. Abe, T. Nogami, The phenolation of monomeric compound of condensed tannins by Lewis acid catalyst, Mokuzai Gakkaishi 38 (1992) 565–592.
[22] T. Mitsunaga, I. Abe, T. Nogami, The formation of a ring-opened compound from (+)-catechin by BF_3 catalyst, Mokuzai Gakkaishi 93 (1993) 328–332.
[23] T. Mitsunaga, I. Abe, T. Nogami, The chemical structure and stereochemistry of the phenol adduct compound derived from (+)-catechin upon phenolation, Mokuzai Gakkaishi 38 (1994) 100–106.
[24] O. Korver, C.K. Wilkins, Circular dichroism spectra of flavanols, Tetrahedron 27 (1971) 5459–5465.
[25] Z. Han, S.L. Bonnet, J.H. Van der Westhuizen, Photochemistry synthesis. Part 1. Synthesis of xanthine derivatives by photolysis of 1-(5′-oxohexyl)-3,7-dimethyl-3,7-dihydro-1H-purine-2,6-dione (pentoxifylline): an ambident chromophore, Tetrahedron 64 (2008) 2619–2625.
[26] J.R. Lakowicz, Principles of Fluorescence Spectroscopy, vol. 1, Springer Science + Business Media, New York, 2006, p. 260.
[27] T.G. Fourie, D. Ferreira, D.G. Roux, Flavonoid synthesis based on photolysis of flavan-3-ols, 3-hydroxyflavanones, and 2-benzylbenzofuranes, J. Chem. Soc. Perkin Trans. I (1977) 125–133.
[28] A.K. Zarkadis, V. Georgakilas, G.P. Perdikomatis, A. Trifonov, G.G. Gurzadyan, S. Skoulika, M.G. Siskos, Triplet- vs. singlet-state imposed photochemistry. The role of substituent effects on the photo-fries and photodissociation reaction of triphenylmethyl silanes, Photochem. Photobiol. Sci. 4 (2005) 469–480.
[29] D. Stadler, A. Goeppert, G. Rasul, G.A. Olag, G.K. Surya Prakash, T. Bach, Chiral benzylic carbocations: low temperature NMR studies and theoretical calculations, J. Org. Chem. 74 (2009) 312–318.
[30] C. Diedrich, S.J. Grimme, Systematic investigation of modern quantum chemical methods to predict circular dichroism spectra, J. Phys. Chem. A 107 (2003) 2524–2539.
[31] T.D. Crawford, M.C. Tam, M.L. Abrams, The current state of *ab initio* calculations of optical rotation and electronic circular dichroism spectra, J. Phys. Chem. A 111 (2007) 12058–12068.
[32] P.J. Stephens, F.J. Devlin, F. Gasparrini, A. Ciogli, D. Spinelli, B.J. Cosimelli, Determination of the absolute configuration of a chiral oxadiazol-3-one calcium channel blocker, resolved using chiral chromatography, via concerted density functional theory calculations of its vibrational circular dichroism, electronic circular dichroism and optical rotation, J. Org. Chem. 72 (2007) 4707–4715.
[33] Y. Ding, X.-C. Li, D. Ferreira, Theoretical calculation of electronic circular dichroism of the rotationally restricted 3,8-biflavonoid morelloflavone, J. Org. Chem. 72 (2007) 9010–9017.
[34] N. Berova, L.D. Bari, G. Pescitelli, Application of electronic circular dichroism in configurational and conformational analysis of organic compounds, Chem. Soc. Rev. 36 (2007) 914–931.
[35] Y. Ding, X.-C. Li, D. Ferreira, 4-Arylflavan3-ols as proanthocyanidin models: absolute configuration via density functional calculation of electronic circular dichroism, J. Nat. Prod. 73 (2010) 435–440.
[36] Y. Ding, X.-C. Li, D. Ferreira, Absolute configuration via density functional calculations of electronic circular dichroism, J. Nat. Prod. 72 (2009) 327–335.